Research Journal of Pharmaceutical, Biological and Chemical Sciences

Microbial Gas sensing property of Pseudomonas aeruginosa with mixed metal catalyst MgFe$_2$O$_4$

Sachin Bangale*[1], Vinay Chaugule[2], Reshma prakshale[1], and Sambhaji Bamane[1]

[1] Metal Oxide Research Laboratory, Determent of Chemistry, Dr. Patangrao Kadam Mahavidyalaya Sangli (M.S.) India.
[2] Determent of Microbiology, Miraj Mahavidyalaya miraj Sangli (M.S.) India

ABSTRACT

Semiconductive nanoparticles of bacteria as *Pseudomonas aeruginosa* with catalyst MgFe$_2$O$_4$ bio film was synthesized by using solution combustion technique. The process was convenient, environment friendly and efficient method. Materials were characterized by TG/DTA, XRD, and TEM. Thick biofilm of *Pseudomonas aeruginosa* MgFe$_2$O$_4$ was measured by exposing it to reducing economical gases. It was found that the *Pseudomonas aeruginosa* was sensors exhibited various sensing responses to these gases at different operating temperature. The sensor exhibited a fast response and a good recovery. The biofilm can be used as a new type of gas-sensing material which has a high sensitivity and good selectivity to various gases at low ppm.

Keywords: Nanostructure *Pseudomonas aeruginosa* with catalyst MgFe$_2$O$_4$, XRD, SEM, TEM, Gas sensor.

*Corresponding author

INTRODUCTION

Pseudomonas aeruginosa is found in soil, water, skin flora, and most man-made environments throughout the world. It thrives not only in normal atmospheres, but also in hypoxic atmospheres, many natural and artificial environments. It uses a wide range of organic material for food; in animals, the versatility enables the organism to infect damaged tissues or those with reduced immunity. It is also able to decompose hydrocarbons and has been used to break down tarballs and oil from oil spills, as well as its ability to grow up to 42°C. Pseudomonas aeruginosa is a gram-negative, rod-shaped, asporogenous, and monoflagellated bacterium that has an incredible nutritional versatility. P. aeruginosa groups tend to form biofilms, which are complex bacterial communities that adhere to a variety of surfaces, including metals, plastics, medical implant materials, and tissue. Biofilms are characterized by "attached for survival" because once they are formed, they are very difficult to destroy. All species and strains of Pseudomonas are Gram-negative rods, and have historically been classified as strict aerobes. Exceptions to this classification have recently been discovered in Pseudomonas biofilms. [34]. A significant number of cells can produce exopolysaccharides known as biofilms. Secretion of exopolysaccharide such as alginate [35].

Depending on their locations, biofilms can either be beneficial and detrimental to the environment. For instance, the biofilms found on rocks and pebbles underwater of lakes and ponds are an important food source for many aquatic organisms. It is about 1-5 µm in length and about 0.5-1.0 µm in breadth, therefore Pseudomonas aeruginosa act as best nanoparticle and therefore used for study along with $MgFe_2O_4$ as a catalyst. Spinal of the type $M^{2+} M_2^{3+}O_4$ attract the research interest because of their versatile practical application [1-2]. Spinel ferrites with the general formula AFe_2O_4 (A = Mn, Co, Ni, Mg, or Zn) are very important magnetic materials because of their interesting magnetic and electrical properties with chemical and thermal stabilities [3]. Magnesium ferrite ($MgFe_2O_4$) is one of the most important ferrites. It has a cubic structure of normal spinel-type and is a soft magnetic n-type semiconducting material, which finds a number of applications in heterogeneous catalysis, adsorption, sensors, and in magnetic technologies [4-5]. Recently, nanostructures of magnetic materials have received more and more attention due to their novel material properties that are significantly different from those of their bulk counterparts [6-9]. Current years have been increased interests in study the gas sensing properties of ferrites [10-12]. Gopal reddy et al. reported the response of copper ferrite ($CuFe_2O_4$) and zinc ferrite ($ZnFe_2O_4$) for hydrogen sulfide (H_2S) and that of nickel ferrite ($NiFe_2O_4$) for chlorine gas (Cl_2) [10]. One of the present authors (Y-L.Liu) was confirmed that $ZnFe_2O_4$ gas sensor has sensing properties for H_2S gas [11]. Magnesium ferrite ($MgFe_2O_4$) is one of the important ferrites with spinel structure [13]. It is used as a catalyst [14] and humidity sensor [15]. It is also an n-type semiconductor with the band gap of 2.18V [16].

The need for a novel gas sensor capable of providing reliable operation in harsh environment is now greater than ever. Such sensors find a range of application, including the monitoring of traffic pollutants or food quality with specially designed electronic noses [17-18]. Gas sensors based on metal oxides are commonly used in the monitoring of toxic pollutants and

can provide the necessary sensitivity, selectivity and stability required by such system [19]. Commonly used oxides include zinc oxide, titanium dioxide, iron oxide, tungsten oxide and tin oxide. These materials have successfully been employed to detect a range of gas vapours, particularly ethanol, methanol and propanol [20-21].

Among various materials used for sensing application, ferrite is used as a good class of sensing materials. But they suffer a drawback of being at higher temperature [22]. Consequently, it is interesting to investigate the gas-sensing properties of $MgFe_2O_4$. The gas sensing efficiency of the materials depends on its microstructural properties which are related to its method of preparation, the later plays a very important role with regard to the chemical, structural and properties of a spinel ferrite. $MgFe_2O_4$ is routinely synthesized by combustion method of precursors zinc nitrate, magnesium nitrate and glycine as fuel [23]. Some alternative number of wet methods including coprecipitation [24], sol-gel [25], microemulsions [26], oxidation techniques [27] and hydrothermal synthesis [28] has been employed for preparation of oxide. An ideal process should be environmentally friendly and should be as simple as possible. A novel preparation technique of nanomaterial combustion synthesis at ambient conditions has been developed to prepared nanosized compounds. It was a high-yielding, low-cost and facile synthesis method. In this study, the powder of nanoparticles Pseudomonas aeruginosa was prepared and mixed with $MgFe_2O_4$ nanoparticles. The $MgFe_2O_4$ nanoparticles was synthesized by novel combustion reaction. One of our aims is to develop a general synthesis method and explore the gas sensing properties of Pseudomonas aeruginosa with catalyst $MgFe_2O_4$ which act as nanopowder. The grain size of $MgFe_2O_4$ is about 15-35nm and size of Pseudomonas aeruginosa is 0.5μ. Furthermore, the Pseudomonas aeruginosa with catalyst $MgFe_2O_4$ biofilm act as gas sensor and has possessed excellent gas-sensing responses to various reducing gases. We found that the process has convenient, environment friendly, inexpensive and efficient. The discovery could aid that, this is low cost process carried out at room temperature particularly for the detection of ammonia gas.

EXPERIMENTAL

Isolation of Pseudomonas aeruginosa

For isolation of Pseudomonas aeruginosa, soil is the raw material used because soil is the chief source for Pseudomonas aeruginosa. One loop full sample from diluted soil was stricted on sterilized Nutrient agar plate, Plate was incubated at 37^0C for 24 hrs. After 24hrs dry blue coloured colony indicates primary confirmation of **Pseudomonas aeruginosa** these colonies are selected for the final confirmation of Pseudomonas aeruginosa.

Confirmation of Pseudomonas aeruginosa

Isolated Pseudomonas aeruginosawas confired by biochemical test. The isolated colony was showing positive results for no of biochemical tests which was indicating presence of Pseudomonas aeruginosa.

Enrichment of Pseudomonas aeruginosa

The confirmed colony were streaked on another nutrient agar plates for enrichment purpose. All plates were incubated at 37^0C for 24 hrs. After 24hrs of incubation, aseptically scrub the growth of Pseudomonas aeruginosa in distilled water. The growth was then centrifuged to get pellet of Pseudomonas aeruginosa.

Powder preparation of Pseudomonas aeruginosa

The pellet of Pseudomonas aeruginosa was allowed to dry and directly use as powder act as nanoparticles. The size of Pseudomonas aeruginosais just about 0.5µm therefore Pseudomonas aeruginosa act as best nanopartical was used for this study.

Powder preparation for MgFe$_2$O$_4$

In this study polycrystalline MgFe$_2$O$_4$ powder was prepared using combustion technique. The materials used as precursors were magnesium nitrate hexahydrate Mg $(NO_3)_2.6H_2O$, iron nitrate hexahydrate $Fe(NO_3)_26H_2O$ and glycine (all these were purchased from AR Grade of Qualigen fine Ltd.India). All of them were of high purity (99.9%, 98%, and 99.9% respectively). Glycine possesses a high heat of combustion. It is an organic fuel providing a platform for redox reactions during the course of combustion. Initially the magnesium nitrate, iron nitrate and glycine was taken in the proportion of 1:1:4 respectively. These proportions were dissolved in a beaker and slowly stirring by using glass rod till clear solution was obtained. Then formed solution was evaporated on hot plate in the temperature range of 70^0C to 80^0C resulting thick gel. The gel was kept on a hot plate for auto combustion and heated in the temperature range of 170^0C to 180^0C.The nanocrystalline MgFe$_2$O$_4$ powder was formed within a few minutes and it was sintered at about 500^0C, 600^0C, 700^0C, and 800^0C for about 4h, it gives brown colour shining powder to nanocrystalline MgFe$_2$O$_4$[29].

Characterization of MgFe2O4 Techniques

The prepared samples were characterized by TG/DTA thermal analyzer (SDT Q600 V 20.9 Build 20), XRD Philips Analytic X-ray B.V. (PW-3710 Based Model diffraction analysis using Cu-K$_\alpha$ radiation), A JEOL JEM–200 CX transmission electron microscope operating at 200 kV analysis.

Thick Film Preparation

The thixotropic paste of powder form of nanocrystalline Pseudomonas aeruginosa and MgFe$_2$O$_4$ was screen printed on a glass substrate in desired patterns. The films prepared were fired at 37^0C for 4 h. Silver contact were made by vacuum evaporation for electrical measurements.
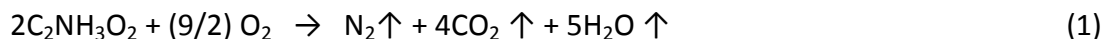
Fabrication and analysis of gas sensors

The sensing performance of the sensors was examined using a "static gas-sensing system. There were electrical feeds through the base plate. The heating wire was fixed on the base plate to heat the sample under test up to the required operating temperatures. The current passing through the heating element was monitored using a relay with adjustable ON and OFF time intervals. Cr-Al thermocouple was used to sense the operating temperature of the sensors. The output of the thermocouple was connected to digital temperature indicators. Gas inlet valve was fitted at one port of the base plate. The required gas concentration inside the static system was achieved by injecting a known volume of test gas using a gas-injecting syringe. Constant voltage was applied to the sensors, and current was measured by a digital Pico-ammeter. Air was allowed to pass into the glass dome after every gases exposure cycle.

RESULT AND DISCUSSION

Spinel structure and formation analysis

The TG curve in Fig. 1 shows a minor weight loss step (20%) from 30 up to about 270^0C and two major weight loss steps from 270 to 455^0C (60%). No further weight loss was observed up to 1000^0C. The minor weight loss was related to the loss of moisture and trapped solvent (water and carbon dioxide) in the as-spun $MgFe_2O_4$ nanopowder, whereas the major weight loss was due to the combustion of organic matrix. On the DTA curve, main exothermic peaks were observed at ~290 and ~ 450^0C, suggesting the thermal events related to the decomposition of Mg and Fe nitrates along with the degradation by dehydration on the nanopowder, which was confirmed by a dramatic weight loss in TG curve at the corresponding temperature range (270–455^0C). The plateau formed between 455 and 1000^0C on the TG curve indicated the formation of crystalline $MgFe_2O_4$ as the decomposition product. As confirmed by XRD and FT-IR analyses as showed in Figs. 2 and 5 respectively. Represented by following reaction (1,2).

$$2C_2NH_3O_2 + (9/2) O_2 \rightarrow N_2\uparrow + 4CO_2 \uparrow + 5H_2O \uparrow \tag{1}$$

$$Mg (NO_3)_3 + Fe (NO_3)_3 + 4C_2H_5NO_2 \rightarrow MgFe_2O_4 + 8CO_2\uparrow + 10H_2O\uparrow + 5N_2\uparrow \tag{2}$$

XRD study:

The XRD patterns of the calcined $MgFe_2O_4$ are shown in Fig. 2. All of the main peaks are indexed as the spinel $MgFe_2O_4$ in the standard data (JCPD No: 88-1935). The average crystallite sizes of $MgFe_2O_4$ samples were calculated from X-ray line broadening of the reflections of (220), (311), (400), (511), and (440) using Scherrer's equation (i.e., $D = 0.89k/(\beta \cos\theta)$, where k is the wavelength of the X-ray radiation, K is a constant taken as 0.89, h the diffraction angle, and b is the full width at half-maximum [30] , and were found to be 16 ± 4, 18 ± 1, 25 ± 2, and 26 ± 3 nm for the samples of $MgFe_2O_4$ calcined at 500, 600, 700, and 800^0C, respectively.
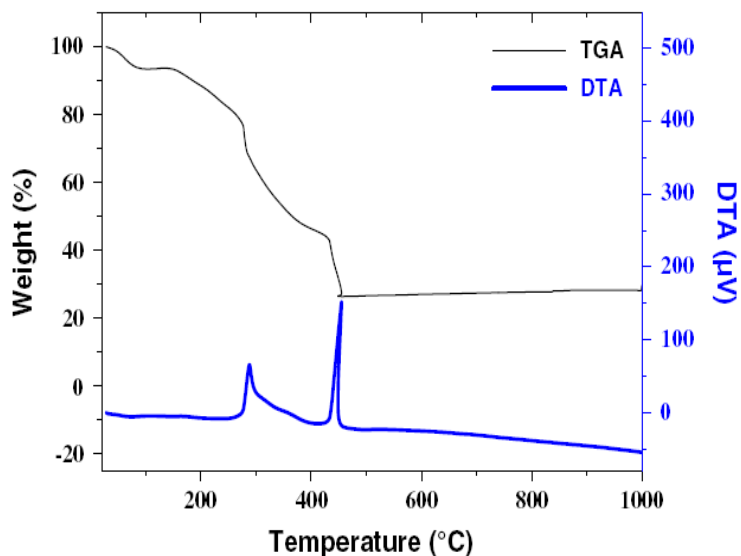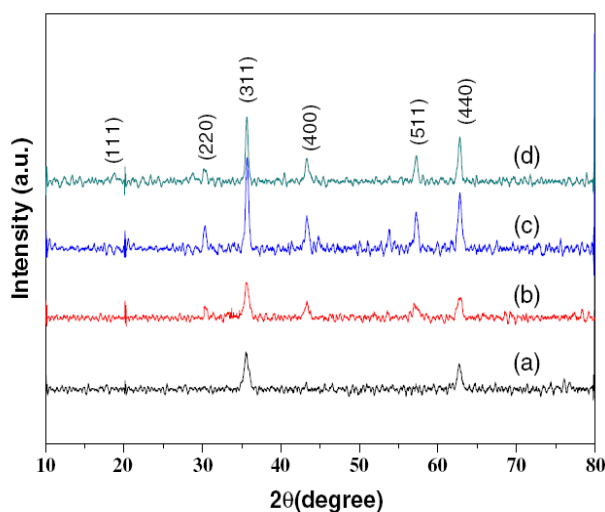
Fig 1: TG-DTA curve of mixed precursor MgFe$_2$O$_4$.

Fig 2: XRD pattern of calcinied mixed precursor MgFe$_2$O$_4$ at a - 500^{0}C, b- 600^{0}C, c-700^{0}C and d- 800^{0}C in air for 4 h.

Particle size distribution studies:

Fig. 3 has been carried out by using dynamic light scattering techniques. (DLS via Laser input energy of 632 nm) It was observed that magnesium iron oxide nanoparticles have narrow size distribute within the range of about 10-15 nm. Which are well match with calculated value and was calculated it from Debye-Scherrer equation.

Fig 3: Particle size distribution studies.

TEM studied:

The detailed morphology and crystalline structure of the MgFe$_2$O$_4$ calcined at 700 and 800^{0}C for 4 h were further investigated by TEM, and the TEM bright-field images with corresponding selected-area electron diffraction (SAED) patterns of these two samples are shown in Fig.4. It is clearly seen from the TEM bright field images that both samples consisted of packed MgFe$_2$O$_4$ particles or crystallites with particle sizes of ~10–20 and 25–80 nm in diameter for the samples of 700^{0}C-calcined and 800^{0}C-calcined, respectively. It is seen that the particle sizes of MgFe$_2$O$_4$ contained in the calcined MgFe$_2$O$_4$ are quite uniform. Since the electro spun powder were very standard data (JCPDS: 88-1935). The diffraction rings are identified as the (111), (220), (311), (400), (422), (511), and (440) planes. This concurs with the results of XRD presented in Fig. 2.
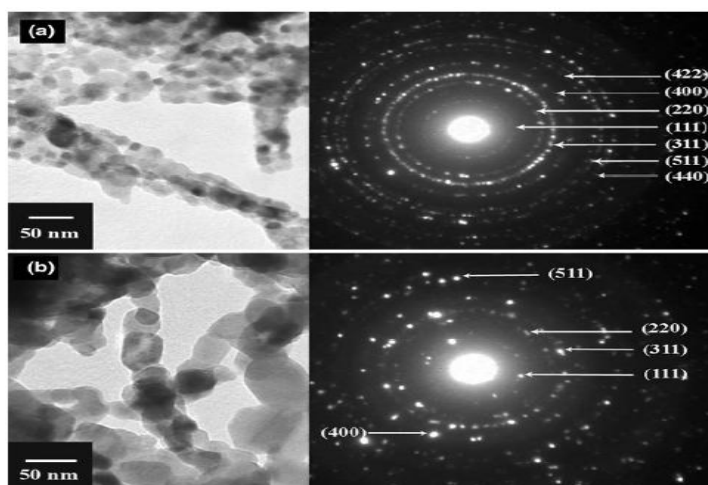
Fig 4: TEM images with corresponding SAED patterns of the MgFe$_2$O$_4$ samples calcined in air for 4 h at a 700^{0}C and b 800^{0}C.

FT-IR Studied:

The formation of spinel MgFe$_2$O$_4$ structure in the calcined MgFe$_2$O$_4$ was further supported by FT-IR spectra (Fig.5). Here, we consider two ranges of the absorption bands: 4000–1000 and 1000–400 cm^{-1} as suggested by previously published studies [31-32]. In the range of 4000–1000 cm^{-1}, vibrations of CO$_3^{2-}$ and moisture were observed. The intensive band at~1627 cm^{-1} is due to O–H stretching vibration interacting through H bonds. The band at ~ 2920 cm^{-1} is C–H asymmetric stretching vibration mode due to the –CH$_2$– groups of the long aliphatic alkyl groups. The υ(C=O) stretching vibration of the carboxylate group (CO$_2^{2-)}$) was observed around 1380 cm^{-1} and the band at ~1016 cm^{-1} was corresponded to nitrate ion traces. Therefore the CO$_3^{2-}$ and CO$_3^-$ vibrations disappeared when calcinations temperature was increased. In the range of 1000– 400cm^{-1}, a typical metal–oxygen absorption band for the spinel structure of the ferrite at ~560 cm^{-1} was observed in the FT-IR spectra of all of the calcined MgFe$_2$O$_4$ samples. This band strongly suggests the intrinsic stretching vibrations of the metal (Fe ↔ O) at the tetrahedral site [33].
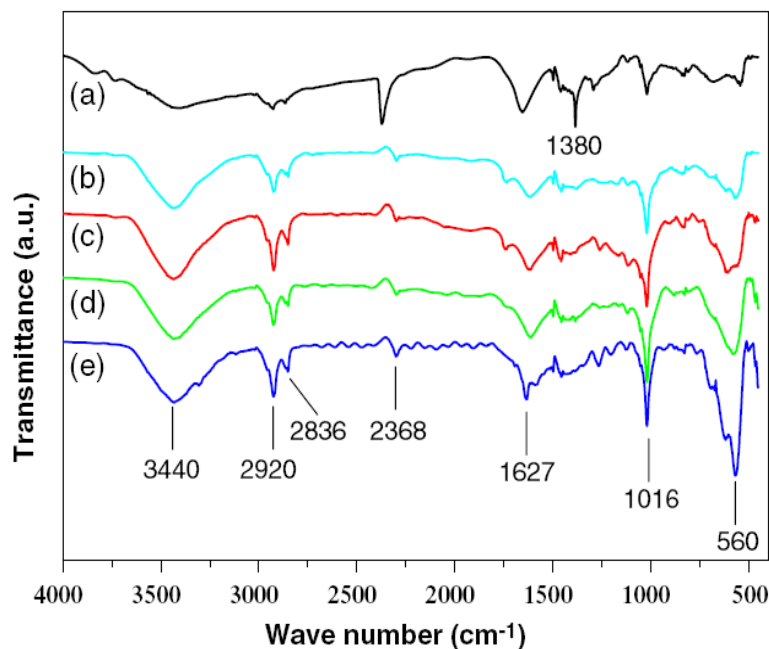

Fig 5: FT-IR spectra of the MgFe$_2$O$_4$ composite samples calcined in air for 4 h at different temperatures. (a) -180^{0}C, (b) -500^{0}C, (c) - 600^{0}C, (d) - 700^{0}C, and (e) - 800^0 C.

ELECTRICAL PROPERTIES

I-V characteristics of thick film nanoparticles Pseudomonas aeruginosa and MgFe$_2$O$_4$

Fig.6 depicts I-V characteristics of nanoparticles Pseudomonas aeruginosa and $MgFe_2O_4$ films. It is clear from the symmetrical I-V characteristics that the silver contacts on the films were ohmic in nature.

Electrical conductivity

Fig.7 shows the variation of log (conductivity) with temperature. The conductivity values of sample increase with operating temperature. The increase in conductivity with increasing temperature could be attributed to negative temperature coefficient of resistance and semiconducting nature of Pseudomonas aeruginosa and $MgFe_2O_4$. It is observed from fig. 7 that the electrical conductivities of the Pseudomonas aeruginosa and $MgFe_2O_4$ films are nearly linear in the temperature range from 30- 40^0C in air ambient.
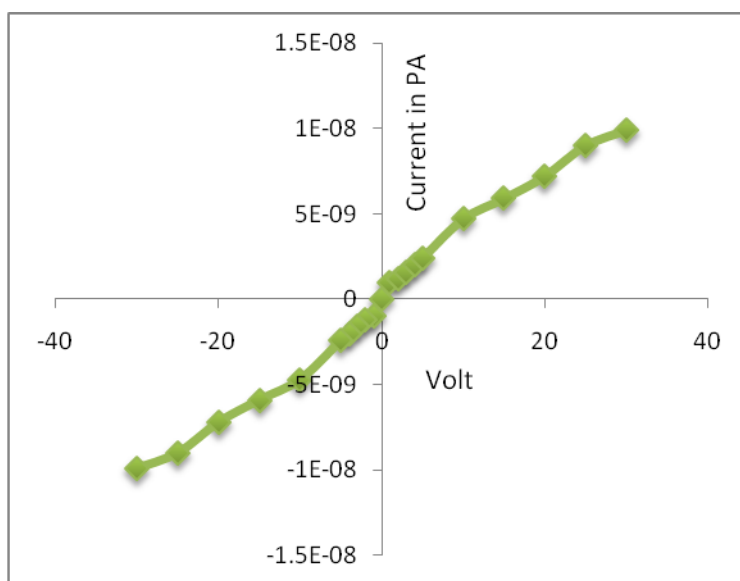

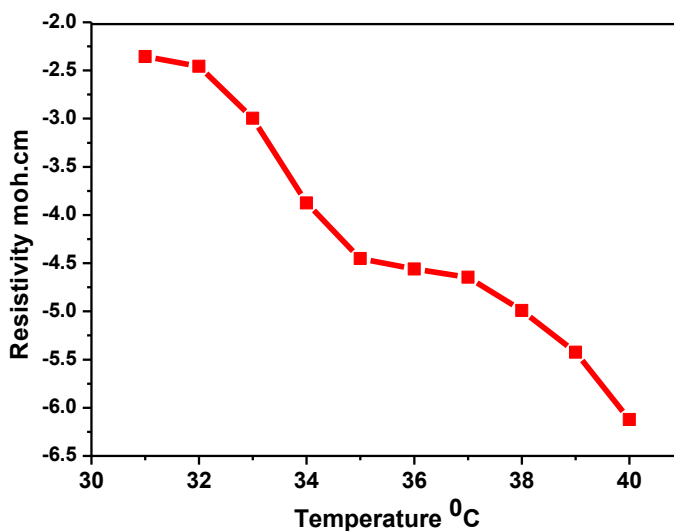**Fig 6: I-V characteristics of the sensor.**

Fig 7: Resistivity Variation of Pseudomonas aeruginosa and MgFe$_2$O$_4$ with reciprocal operating temperature.

SENSING PERFORMANCE OF THE SENSOR

Measurement of gas response, selectivity, response and recovery time

Gas response (S) is defined as the ratio of the change in conductance of the sensor on exposure to the target gas to the original conductance in air. The relation for S is as:

$$S = \frac{G_g - G_a}{G_a}$$

where G_a and G_g are the conductance of sensor in air and in a target gas medium, respectively.

Selectivity or specificity is defined as the ability of a sensor to respond to a certain gas in the presence of other gases.

The time taken for the sensors to attain 90% of the original conductance is the recovery time.

Sensing performance of thick film Pseudomonas aeruginosa and MgFe$_2$O$_4$

Effect of operating temperature

Table 1 and Fig. 8 depict the variation response of Pseudomonas aeruginosa to H_2S (1000 ppm) with various operating temperature. The largest response of nanaopartical Pseudomonas aeruginosa $Mg_2Fe_2O_4$ thick film was observed to be 6.70 at 37^0C. The H_2S response at 37^0C temperature was expected to be monitored by adsorption of moisture on the Pseudomonas aeruginosa, $MgFe_2O_4$ film. The cumulative effect would decrease the film resistance, giving a response to H_2S gas at 37^0C. Except 37^0C, there would be no more oxygen adsorption. Therefore, the oxygen adsorption-desorption mechanism is quit employed to sense the H_2S gas at other temperature.

Table 1: Variations of various gas responses to Pseudomonas aeruginosa and MgFe$_2$O$_4$ thick film with operating temperatures

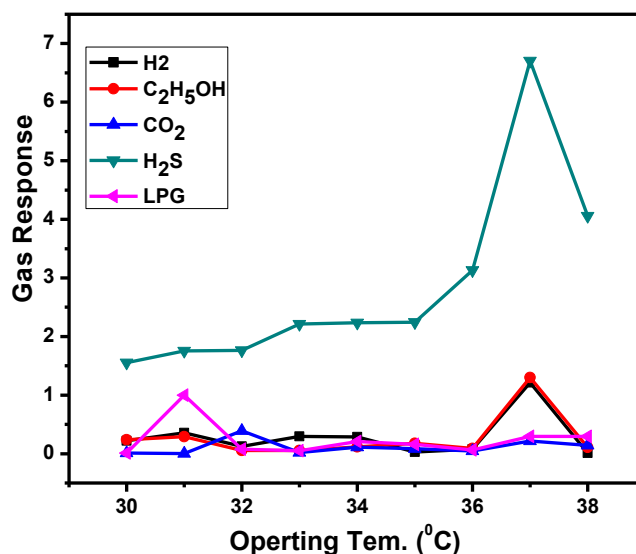| Temperature	H_2	C_2H_5OH	CO_2	H_2S	LPG
38	0.01	0.1052	0.1428	4.0555	0.29411
37	1.213	1.302	0.21818	6.7065	0.2951
36	0.0746	0.08823	0.04412	3.13285	0.06493
35	0.0304	0.17931	0.08695	2.245	0.16
34	0.2875	0.11428	0.1111	2.2337	0.2058
33	0.2958	0.05408	0.0204	2.2137	0.05194
32	0.123	0.05405	0.3896	1.7647	0.07812
31	0.355	0.29082	0.0012	1.7547	1.00
30	0.221	0.24	0.012	1.553	0.01

Fig 8: Graphical variations of various gas responses to Pseudomonas aeruginosa and MgFe$_2$O$_4$ thick film with different operating temperatures.

Effect of H$_2$S gas concentration at 37^{0}C (Active Region)

The variation of gas response of the Pseudomonas aeruginosa MgFe$_2$O$_4$ sample with H$_2$S gas concentration at 37^{0}C is represented in Fig.9. This film was exposed to varying concentrations of H$_2$S gas. For thick film of Pseudomonas aeruginosa MgFe$_2$O$_4$, the response values were observed to increase continuously with increasing the gas concentration up to 30 ppm at 37^{0}C. The rate of increase in response was relatively larger up to 30 ppm , but smaller during 30 and 1000 ppm. Thus, the active region of the sensors would be up to 30 ppm. At lower gas concentration, the unimolecular layer of gas molecules would be formed on the surface of the sensor which could interact more actively giving larger response. The multilayer of the gas molecules on the sensor surface, at the higher gas concentration, would result into saturation in response beyond 30 ppm gas.
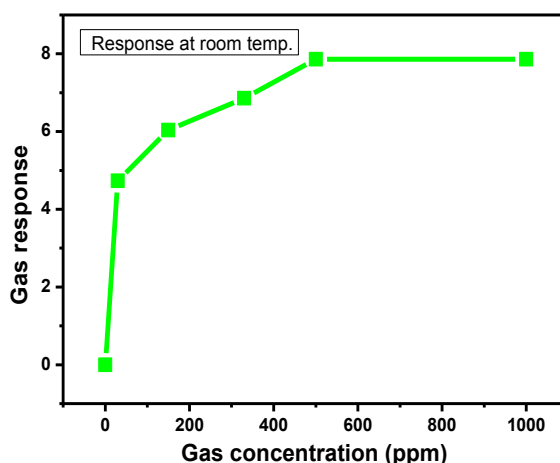

Fig 9: Variation of gas response with gas concentration.

Selectivity for H$_2$S against various gases

Fig.10. depicts the selectivity of the Pseudomonas aeruginosa MgFe$_2$O$_4$ sensor for H$_2$S (30 ppm) gas at 37^{0}C. The sensor showed high selectivity to H$_2$S at 30 ppm and 37^{0}C temperature against other gases ethanol, CO$_2$, H$_2$ and LPG gases but these gases showed high selectivity at 1000 ppm.

Response and recovery of the sensor

Fig.11 depicts the response and recovery of the Pseudomonas aeruginosa MgFe$_2$O$_4$ sensor. The response was quick (~ 17 s) to 30 ppm of H$_2$S, while the recovery was considerably

fast (~ 55s). A negligible quantity of the surface reaction product and its volatility explain its quick response to H_2S and fast recovery to its initial chemical status.
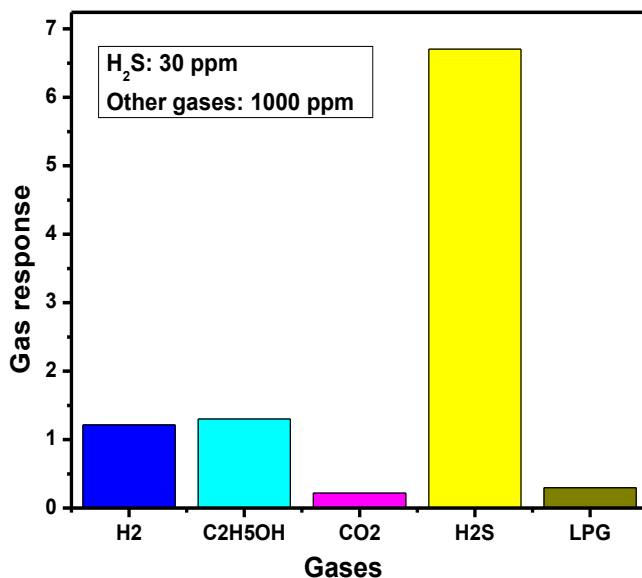

Fig 10: Selectivity of Pseudomonas aeruginosa MgFe$_2$O$_4$ thick film among various gases.
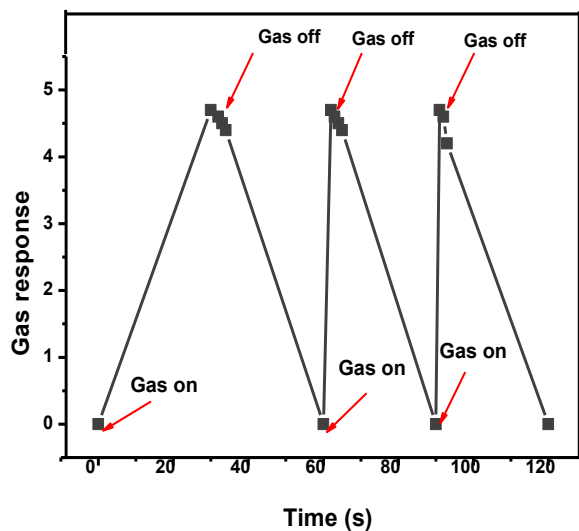

Fig 11: Response and recovery of the sensors.

Response at various temperature

The Pseudomonas aeruginosa $MgFe_2O_4$ thick films cause the formation of intergrain boundaries of Pseudomonas aeruginosa-$MgFe_2O_4$-Pseudomonas aeruginosa-$MgFe_2O_4$ grains. The exposed all gases molecule captures the lattice oxygen from the surface of the film at various temperature. This would result the oxygen deficiency in the bulk of the material preferably at the surface. The semiconductivity in Pseudomonas aeruginosa $MgFe_2O_4$ may be due to large oxygen deficiency. The increase in the conductivity of Pseudomonas aeruginosa $MgFe_2O_4$ thick film could be attributed to the charge-carrier generation mechanism resulted from the electronic defects due to nanostructured size of the grains. These generated electrons and the donor level in the energy band gap of Pseudomonas aeruginosa $MgFe_2O_4$ will contribute to increase in conductivity. This results in increasing the conductance of the film at various temperatures.

CONCLUSIONS

(I) Pseudomonas aeruginosa use as nano crystalline material synthesized by centrifuged and dried method and nanocrystalline $MgFe_2O_4$ has been synthesized by self combustion route. This synthesis route may be used for the synthesis of other metal oxide.

(II) These nanoparticles which show good I-V characteristics with ideal semiconducting nature.

(III)Among all other additives tested, Pseudomonas aeruginosa $MgFe_2O_4$ is outstanding in promoting the H_2S gas.

(IV) Pseudomonas aeruginosa $MgFe_2O_4$ to be optimum and showed highest response to H_2S at 37^0C.

(V)The sensor showed very rapid response(~17) and recovery(~55) to H_2S gas.

(VI) The sensor has good selectivity to H_2S against ethanol, Hydrogen, CO_2, and LPG also.

ACKNOWLEDGEMENTS

REFERENCES

[1]   Sugimoto M. J Am Ceram Soc 1999; 82: 269.
[2]   Liu Y, Liu ZM, Yang Y, Yang HF, Shen GL, Yu RQ. Sensors ans Actuators B 2005; 107: 600-604.
[3]   Hankare PP, Jadhav SD, Sankpal UB, Patil RP, Sasikala R, Mulla IS. Alloys and Compounds 2009; 488: 270-272.
[4]   Willey RJ, Noirclerc P, Busca G. Chem Eng Commun 1993; 123.
[5]   Oliver SA, Willey RJ, Hamdeh HH, Oliveri G, Busca G. Scr Mater 1995; 33: 1695.
[6]   Wu W, He Q, Jiang C. Nanoscale Res Lett 2008; 3: 397.
[7]   Hua ZH, Chen RS, Li CL, Yang SG, Lu M, Gu XB, Du YW. J Alloys Compd 2007; 427: 199.
[8]   Corr SA, Rakovich YP, Gun'ko YK. Nanoscale Res Lett 2008; 3:87.
[9]   Lai Z, Xu G, Zheng Y. Nanoscale Res Lett 2007; 2: 40.

[10] Gopal Reddy CV, Manorama SV, Rao VJ. J Mater Sci Lett 2000; 19: 775.

[11] Xinshu N, Yanli L, X Jiaqiang. Chin Funct Mater 2002; 33: 413.

[12] Satyanarayana L, Madhusudan K, Reddy VM, Sunkara. Mater Chem Phys 2003; 82: 21.

[13] Liu C, Zou B, Rondinone AJ, Zhang ZJ. J Am Chem Soc 2000; 122: 6263.

[14] Busca G, Finocchio E, Lorenzelli V, Trombetta M, Rossini SA. J Chem Soc Faraday Trans 1996; 92: 4687.

[15] Shimizu Y, Arai H, T Seiyama. Sens Actuators 1985; 7: 11.

[16] Benko FA, Koffyberg FP. Mater Res Bull 1986; 21: 1183.

[17] Sugimoto M. J Am Ceram Soc 1999; 82: 269-280.

[18] Kamble RB, Mathe VL. Sensors and Actuatora B 2008; 131: 205-209.

[19] McMichael RD, Shull RD, LJ Swartzendruber, Bennett LH, Watson RE. J Magn Magn Mater 1992; 11: 29-33.

[20] Gopal Reddy CV, Manorama SV, Rao VJ. J Mater Sci Lett 2000; 9:775-778.

[21] Chen NS, Yang XJ, Liu ES, Huang JL, Sens Actuators B 2000; 66:178180.

[22] Rezlescu E, Popa PD, N Rezlescu 2006; 8: 1016.

[23] Khetre SM, Jadhav HV, Jagdale PN, Bangale SV, Bamane SR. Advances in Applied Science Research 2011; 2(2): 252-259.

[24] Kodama T, Wada Y, Yamamoto T, Tsuji M. J Mater Chem 1995; 5:1413.

[25] Bangale SV, Patil DR, Bamane SR. Sensors & Transducers Journal 2011; 134(11): 107-119.

[26] Hochepied JF, Bonville P, Pileni MP. J Phys Chem B 2000; 104:905.

[27] Kiyama M. Bull Soc Jpn 1978; 51: 134.

[28] Bangale SV, Patil DR, Bamane SR. Sensors & Transducers Journal 2011; 134(11): 95-106.

[29] Bangale SV, Khetre SM and Bamane SR. Advances in Applied Science Research 2011; 2: 252-259.

[30] Cullity BD, Stock SR. Elements of X-ray Diffraction Prentice Hall, NJ, 2001.

[31] Huang Y, Tang Y, Wang J, Chen Q. Mater Chem Phys 2006; 97:394.

[32] Pradeep A, Chandrasekaran G. Magnesium Mater Lett 2006; 60:371.

[33] Rao GVS, Rao CNR, Ferraro JR Appl Spectrosc 1970; 24:436.

[34] Hassett D, Cuppoletti J, Trapnell B, Lymar S, Rowe J, Yoon S, Hilliard G, Parvatiyar K, Kamani M, Wozniak D, Hwang S, McDermott T, Ochsner U (2002). Adv Drug Deliv Rev 54 (11): 1425–1443.

[35] Ryan KJ; Ray CG (editors). Sherris Medical Microbiology (4th ed.). McGraw Hill 2004.